Charm mixing as input for model-independent determinations of the CKM phase γ ☆

Samuel Harnew *, Jonas Rademacker *

H H Wills Physics Laboratory, Bristol, UK

ARTICLE INFO

ABSTRACT

The coherence factor and average strong phase difference of D^0 and $\bar{D}^0$ decay amplitudes to the same final state play an important role in the precision determination of the CKM parameter γ using $B^{\pm} \to DK^{\pm}$ and related decay modes. So far, this important input from the charm sector could only be obtained from measurements based on quantum-correlated $D\bar{D}$ pairs produced at the charm threshold. We propose to constrain these parameters using charm mixing, using the large charm samples available at the B factories and LHCb. We demonstrate for the example of $D \to K^+\pi^-\pi^+\pi^-$ that a substantial improvement in the precision of the coherence factor and average strong phase difference can be obtained with this method, using existing data.

© 2013 The Authors. Published by Elsevier B.V. All rights reserved.

1. Introduction

In this Letter we present a new method of constraining the coherence factor and average strong phase difference between D^0 and $\bar{D}^0$ decay amplitudes to the same multibody final state [1], using input from charm mixing.

Charm threshold data [2–6] provide important input to the measurement of the charge-parity (*CP*) violating phase γ in $B^{\pm} \to DK^{\pm}$, $B^0 \to DK^*$ and similar decay modes[1] [1,7–12], where the details of the analysis depend considerably on the final state of the subsequent D decay [13–18]. The importance of charm threshold data in this context results from the well-defined superposition states of D^0 and $\bar{D}^0$ accessible with quantum-correlated $D\bar{D}$ pairs.

Charm mixing [19–25] also provides well-defined D^0–$\bar{D}^0$ superposition states, which can be used in a similar manner. Previous studies indicate that for D decays to self-conjugate final states, like $D \to K_S\pi^+\pi^-$ and $D \to K_S K^+K^-$, datasets much larger than those currently available are required to significantly improve on the existing constraints from the charm threshold [26]. The interference effects due to D mixing in suppressed decay modes such as $D^0 \to K^+\pi^-\pi^+\pi^-$ and $D^0 \to K^+\pi^-\pi^0$ are enhanced compared to self-conjugate decays. We propose to exploit this feature, and demonstrate that a substantial reduction of the uncertainty

on the coherence factor and average strong phase difference in $D \to K^+\pi^-\pi^+\pi^-$ is possible with existing data.

This Letter is structured as follows: In Section 2 we review the mixing formalism for multibody D decays, building on and extending the treatment presented in [27,28]. We present a unified description of the mixing-induced interference effects in decays to self conjugate and non-self conjugate final states. In Section 3 we show how D-mixing can be used to constrain the coherence factor and strong phase difference. Using simulated $D \to K^+\pi^-\pi^+\pi^-$ decays we demonstrate that a substantial improvement in the precision of the coherence factor and average strong phase difference is possible using existing data; here we are guided by the expected signal yields from LHCb's 2011 and 2012 data taking period. In Section 4, we conclude.

2. Mixing formalism

In this section we review the charm mixing formalism for multibody decays and its relationship to the interference parameters relevant for the measurement of γ in $B^{\pm} \to DK^{\pm}$ and similar decay modes [26–28]. We introduce the complex interference parameter $\mathcal{Z}^f$ that unifies the formalism for decays to self-conjugate states [2,3,8] and non self-conjugate states [1,4,5]. $\mathcal{Z}^f$ is also particularly convenient for parameterising the constraints on charm interference effects derived from mixing using suppressed D decay modes, discussed in Section 3. Finally, in this section, we identify the important differences in the formalisms conventionally used for charm mixing measurements on one hand, and $B^{\pm} \to DK^{\pm}$ and related measurements on the other.

---

 * Corresponding author.

 [1] *CP*-conjugate decays are implied throughout, unless stated otherwise. D stands for any superposition of D^0 and $\bar{D}^0$.

2.1. Charm mixing

The mass eigenstates $|D_1^0\rangle$ and $|D_2^0\rangle$, with masses M_1, M_2 and widths Γ_1, Γ_2, are related to the flavour eigenstates $|D^0\rangle$ and $|\bar{D}^0\rangle$ through

$$|D_1\rangle = p|D^0\rangle + q|\bar{D}^0\rangle, \qquad |D_2\rangle = p|D^0\rangle - q|\bar{D}^0\rangle, \qquad (2.1)$$

where p and q are complex numbers that satisfy $|q|^2 + |p|^2 = 1$. We also define

$$M \equiv \frac{M_1 + M_2}{2}, \qquad \Gamma \equiv \frac{\Gamma_1 + \Gamma_2}{2},$$
$$\Delta M \equiv M_2 - M_1, \qquad \Delta\Gamma \equiv \Gamma_2 - \Gamma_1 \qquad (2.2)$$

and the usual dimensionless mixing parameters

$$x \equiv \frac{\Delta M}{\Gamma}, \qquad y \equiv \frac{\Delta\Gamma}{2\Gamma}. \qquad (2.3)$$

The deviation of $|q/p|$ from 1 is a measure of CP violation (CPV) in D-mixing. The phase $\phi_{mix} \equiv \arg(\frac{q}{p})$ is a convention-dependent quantity that is sensitive to CPV in the interference between mixing and decay – usually, a phase convention is chosen where $\phi_{mix} = 0$ in the absence of CPV. In practice we will deal with D mesons that have definite flavour at creation. These evolve over time t to the following superpositions of D^0 and $\bar{D}^0$:

$$|D^0(t)\rangle = g_+(t)|D^0\rangle + \frac{q}{p}g_-(t)|\bar{D}^0\rangle,$$
$$|\bar{D}^0(t)\rangle = g_+(t)|\bar{D}^0\rangle + \frac{p}{q}g_-(t)|D^0\rangle, \qquad (2.4)$$

where $|D^0(t)\rangle$ refers to a state that was pure D^0 at time $t = 0$, while $|\bar{D}^0(t)\rangle$ refers to a state that was purely $\bar{D}^0$ at $t = 0$. The time-dependent functions $g_-(t)$ and $g_+(t)$ are given by

$$g_+(t) = e^{-iMt - \frac{1}{2}\Gamma t}\cos\left(\frac{1}{2}\Delta Mt - \frac{i}{4}\Delta\Gamma t\right),$$
$$g_-(t) = e^{-iMt - \frac{1}{2}\Gamma t}i\sin\left(\frac{1}{2}\Delta Mt - \frac{i}{4}\Delta\Gamma t\right). \qquad (2.5)$$

2.2. The complex interference parameter $\mathcal{Z}^f$

For the decay amplitudes of a D flavour eigenstate to a particular final state f, or its CP conjugate $\bar{f}$, we use the following notation:

$$\mathcal{A}(\mathbf{p}) \equiv \langle f_{\mathbf{p}}|\hat{H}|D^0\rangle, \qquad \bar{\mathcal{A}}(\bar{\mathbf{p}}) \equiv \langle \bar{f}_{\bar{\mathbf{p}}}|\hat{H}|\bar{D}^0\rangle,$$
$$\mathcal{B}(\mathbf{p}) \equiv \langle f_{\mathbf{p}}|\hat{H}|\bar{D}^0\rangle, \qquad \bar{\mathcal{B}}(\bar{\mathbf{p}}) \equiv \langle \bar{f}_{\bar{\mathbf{p}}}|\hat{H}|D^0\rangle. \qquad (2.6)$$

Here $\mathbf{p}$ identifies a point in phase space for the multibody final state f, and $\bar{\mathbf{p}}$ identifies the corresponding point for the CP-conjugate final state, where all final state momenta and charges are reversed. In practice we will integrate over finite phase-space volumes. Following [1] we therefore define[2]

$$\int_\Omega \mathcal{A}(\mathbf{p})\mathcal{A}^*(\mathbf{p})\frac{d\Phi}{d\mathbf{p}}d\mathbf{p} \equiv \mathcal{A}^2, \qquad \int_{\bar{\Omega}} \bar{\mathcal{A}}(\bar{\mathbf{p}})\bar{\mathcal{A}}^*(\bar{\mathbf{p}})\frac{d\bar{\Phi}}{d\bar{\mathbf{p}}}d\bar{\mathbf{p}} \equiv \bar{\mathcal{A}}^2,$$
$$\int_\Omega \mathcal{B}(\mathbf{p})\mathcal{B}^*(\mathbf{p})\frac{d\Phi}{d\mathbf{p}}d\mathbf{p} \equiv \mathcal{B}^2, \qquad \int_{\bar{\Omega}} \bar{\mathcal{B}}(\bar{\mathbf{p}})\bar{\mathcal{B}}^*(\bar{\mathbf{p}})\frac{d\bar{\Phi}}{d\bar{\mathbf{p}}}d\bar{\mathbf{p}} \equiv \bar{\mathcal{B}}^2. \quad (2.7)$$

We use the symbols $\frac{d\Phi}{d\mathbf{p}}$ and $\frac{d\bar{\Phi}}{d\bar{\mathbf{p}}}$ for the density of states at $\mathbf{p}$ and $\bar{\mathbf{p}}$ respectively. The integrals containing $\mathcal{A}(\mathbf{p})$ and $\mathcal{B}(\mathbf{p})$ run over the phase space volume Ω, and the ones containing $\bar{\mathcal{A}}(\bar{\mathbf{p}})$ and $\bar{\mathcal{B}}(\bar{\mathbf{p}})$ run over the CP conjugate volume $\bar{\Omega}$. These volumes can encompass all of phase space, or any part thereof. The interference effects are described by the integrals over the cross terms:

$$\frac{\int_\Omega \mathcal{A}(\mathbf{p})\mathcal{B}^*(\mathbf{p})\frac{d\Phi}{d\mathbf{p}}d\mathbf{p}}{\mathcal{A}\mathcal{B}} \equiv \mathcal{Z}_\Omega^f, \qquad \frac{\int_{\bar{\Omega}} \bar{\mathcal{A}}(\bar{\mathbf{p}})\bar{\mathcal{B}}^*(\bar{\mathbf{p}})\frac{d\bar{\Phi}}{d\bar{\mathbf{p}}}d\bar{\mathbf{p}}}{\bar{\mathcal{A}}\bar{\mathcal{B}}} \equiv \mathcal{Z}_{\bar{\Omega}}^{\bar{f}}. \quad (2.8)$$

This defines the complex interference parameter $\mathcal{Z}_\Omega^f$ for the final state f over the phase space region Ω, and $\mathcal{Z}_{\bar{\Omega}}^{\bar{f}}$, its CP-conjugate. For integrals over all phase space we use $\mathcal{Z}^f$, omitting the subscript. The magnitude of $\mathcal{Z}_\Omega^f$ is between 0 and 1. The phase of $\mathcal{Z}_\Omega^f$ represents a weighted average of the phase difference between the two amplitudes over Ω. The parameter $\mathcal{Z}^f$ is directly related to the coherence factor R_D^f and average phase difference δ_D^f introduced in [1],

$$\mathcal{Z}^f \equiv R_D^f e^{-i\delta_D^f}. \qquad (2.9)$$

For binned analyses in decays to self-conjugate final states such as $K_S\pi^+\pi^-$, these interference effects are usually parametrised instead by c_i and s_i. These are weighted averages of the cosine and the sine of the phase difference between D^0 and $\bar{D}^0$ decay amplitudes, taken over a phase-space bin i covering the volume Ω_i. This formalism was originally introduced in [8]; we follow the definition of c_i and s_i used in most subsequent articles [2,3,9,28,29]. The c_i and s_i parameters are related to the complex interference parameter through

$$\mathcal{Z}_{\Omega_i}^f \equiv c_i + is_i. \qquad (2.10)$$

We will continue to use $\mathcal{Z}_\Omega^f$ as it unifies the formalism for decays to self-conjugate and non-self conjugate states. In terms of the parameters defined above, the time-dependent decay rates are given by

$$\Gamma\left(D^0(t) \to f\right)_\Omega = \frac{1}{2}\left[\mathcal{A}^2(\cosh y\Gamma t + \cos x\Gamma t) \right.$$
$$+ \mathcal{B}^2(\cosh y\Gamma t - \cos x\Gamma t)\left|\frac{q}{p}\right|^2$$
$$+ 2\mathcal{A}\mathcal{B}\left[Re\left(\mathcal{Z}_\Omega^f\frac{q}{p}\right)\sinh(y\Gamma t)\right.$$
$$\left.\left. + Im\left(\mathcal{Z}_\Omega^f\frac{q}{p}\right)\sin(x\Gamma t)\right]\right]e^{-\Gamma t}, \qquad (2.11)$$

$$\Gamma\left(D^0(t) \to \bar{f}\right)_{\bar{\Omega}} = \frac{1}{2}\left[\bar{\mathcal{B}}^2(\cosh y\Gamma t + \cos x\Gamma t) \right.$$
$$+ \bar{\mathcal{A}}^2(\cosh y\Gamma t - \cos x\Gamma t)\left|\frac{q}{p}\right|^2$$
$$+ 2\bar{\mathcal{A}}\bar{\mathcal{B}}\left[Re\left(\mathcal{Z}_{\bar{\Omega}}^{\bar{f}*}\frac{q}{p}\right)\sinh(y\Gamma t)\right.$$
$$\left.\left. + Im\left(\mathcal{Z}_{\bar{\Omega}}^{\bar{f}*}\frac{q}{p}\right)\sin(x\Gamma t)\right]\right]e^{-\Gamma t}, \qquad (2.12)$$

---

[2] Throughout this note * is used to denote the complex conjugate, whereas ¯ is used to denote the CP conjugate.

$$\Gamma\left(\bar{D}^0(t)\to\bar{f}\right)_{\bar{\Omega}} = \frac{1}{2}\Bigg[\bar{\mathcal{A}}^2(\cosh y\Gamma t+\cos x\Gamma t)$$

$$+\bar{\mathcal{B}}^2(\cosh y\Gamma t-\cos x\Gamma t)\left|\frac{p}{q}\right|^2$$

$$+2\bar{\mathcal{A}}\bar{\mathcal{B}}\Bigg[Re\left(\mathcal{Z}_{\bar{\Omega}}^{\bar{f}}\frac{p}{q}\right)\sinh(y\Gamma t)$$

$$+Im\left(\mathcal{Z}_{\bar{\Omega}}^{\bar{f}}\frac{p}{q}\right)\sin(x\Gamma t)\Bigg]\Bigg]e^{-\Gamma t}, \qquad (2.13)$$

$$\Gamma\left(\bar{D}^0(t)\to f\right)_{\Omega} = \frac{1}{2}\Bigg[\mathcal{B}^2(\cosh y\Gamma t+\cos x\Gamma t)$$

$$+\mathcal{A}^2(\cosh y\Gamma t-\cos x\Gamma t)\left|\frac{p}{q}\right|^2$$

$$+2\mathcal{A}\mathcal{B}\Bigg[Re\left(\mathcal{Z}_{\Omega}^{f*}\frac{p}{q}\right)\sinh(y\Gamma t)$$

$$+Im\left(\mathcal{Z}_{\Omega}^{f*}\frac{p}{q}\right)\sin(x\Gamma t)\Bigg]\Bigg]e^{-\Gamma t}. \qquad (2.14)$$

Assuming that terms of order 3 and higher in the mixing parameters x and y are negligible leads to the following expressions:

$$\Gamma\left(D^0(t)\to f\right)_{\Omega}$$
$$\simeq\Bigg[\mathcal{A}^2\left(1+\frac{y^2-x^2}{4}(\Gamma t)^2\right)+\mathcal{B}^2\left(\left|\frac{q}{p}\right|^2\frac{x^2+y^2}{4}(\Gamma t)^2\right)$$
$$+\mathcal{A}\mathcal{B}\left(y\,Re\left(\mathcal{Z}_{\Omega}^{f}\frac{q}{p}\right)+x\,Im\left(\mathcal{Z}_{\Omega}^{f}\frac{q}{p}\right)\right)(\Gamma t)\Bigg]e^{-\Gamma t}, \qquad (2.15)$$

$$\Gamma\left(D^0(t)\to\bar{f}\right)_{\bar{\Omega}}$$
$$\simeq\Bigg[\bar{\mathcal{B}}^2\left(1+\frac{y^2-x^2}{4}(\Gamma t)^2\right)+\bar{\mathcal{A}}^2\left(\left|\frac{q}{p}\right|^2\frac{x^2+y^2}{4}(\Gamma t)^2\right)$$
$$+\bar{\mathcal{A}}\bar{\mathcal{B}}\left(y\,Re\left(\mathcal{Z}_{\bar{\Omega}}^{\bar{f}*}\frac{q}{p}\right)+x\,Im\left(\mathcal{Z}_{\bar{\Omega}}^{\bar{f}*}\frac{q}{p}\right)\right)(\Gamma t)\Bigg]e^{-\Gamma t}, \qquad (2.16)$$

$$\Gamma\left(\bar{D}^0(t)\to\bar{f}\right)_{\bar{\Omega}}$$
$$\simeq\Bigg[\bar{\mathcal{A}}^2\left(1+\frac{y^2-x^2}{4}(\Gamma t)^2\right)+\bar{\mathcal{B}}^2\left(\left|\frac{p}{q}\right|^2\frac{x^2+y^2}{4}(\Gamma t)^2\right)$$
$$+\bar{\mathcal{A}}\bar{\mathcal{B}}\left(y\,Re\left(\mathcal{Z}_{\bar{\Omega}}^{\bar{f}}\frac{p}{q}\right)+x\,Im\left(\mathcal{Z}_{\bar{\Omega}}^{\bar{f}}\frac{p}{q}\right)\right)(\Gamma t)\Bigg]e^{-\Gamma t}, \qquad (2.17)$$

$$\Gamma\left(\bar{D}^0(t)\to f\right)_{\Omega}$$
$$\simeq\Bigg[\mathcal{B}^2\left(1+\frac{y^2-x^2}{4}(\Gamma t)^2\right)+\mathcal{A}^2\left(\left|\frac{p}{q}\right|^2\frac{x^2+y^2}{4}(\Gamma t)^2\right)$$
$$+\mathcal{A}\mathcal{B}\left(y\,Re\left(\mathcal{Z}_{\Omega}^{f*}\frac{p}{q}\right)+x\,Im\left(\mathcal{Z}_{\Omega}^{f*}\frac{p}{q}\right)\right)(\Gamma t)\Bigg]e^{-\Gamma t}. \qquad (2.18)$$

For the remainder of this article we assume, for simplicity, that CPV in charm is negligible, leading to: $|\mathcal{Z}_{\Omega}^f|=|\mathcal{Z}_{\bar{\Omega}}^{\bar{f}}|$, $\mathcal{A}=\bar{\mathcal{A}}$ and $\mathcal{B}=\bar{\mathcal{B}}$ (no direct CPV); $|q/p|=1.0$ (no CPV in mixing); and $\arg(\mathcal{Z}_{\Omega}^f\frac{q}{p})=\arg(\mathcal{Z}_{\bar{\Omega}}^{\bar{f}}\frac{p}{q})$ (no CPV in the interference between mixing and decay). Following the usual phase convention, we set ϕ_{mix} to zero in the absence of CPV in the interference between mixing and decay, leading to $q/p=1$ and $\mathcal{Z}_{\Omega}^f=\mathcal{Z}_{\bar{\Omega}}^{\bar{f}}$. With this, the expressions in Eqs. (2.15)–(2.18) simplify to

$$\Gamma\left(D^0(t)\to f\right)_{\Omega}$$
$$\simeq\Bigg[\mathcal{A}^2\left(1+\frac{y^2-x^2}{4}(\Gamma t)^2\right)+\mathcal{B}^2\left(\frac{x^2+y^2}{4}(\Gamma t)^2\right)$$
$$+\mathcal{A}\mathcal{B}(y\,Re(\mathcal{Z}_{\Omega}^f)+x\,Im(\mathcal{Z}_{\Omega}^f))(\Gamma t)\Bigg]e^{-\Gamma t}, \qquad (2.19)$$

$$\Gamma\left(\bar{D}^0(t)\to f\right)_{\Omega}$$
$$\simeq\Bigg[\mathcal{B}^2\left(1+\frac{y^2-x^2}{4}(\Gamma t)^2\right)+\mathcal{A}^2\left(\frac{x^2+y^2}{4}(\Gamma t)^2\right)$$
$$+\mathcal{A}\mathcal{B}(y\,Re(\mathcal{Z}_{\Omega}^f)-x\,Im(\mathcal{Z}_{\Omega}^f))(\Gamma t)\Bigg]e^{-\Gamma t}, \qquad (2.20)$$

with identical expressions for the *CP*-conjugate processes. Since we have removed all weak phases, $\arg(\mathcal{Z}^f)=-\delta_D^f$ now represents the average *strong* phase difference.

2.3. Conventions

There are two different definitions of the *CP* operator in use. The Heavy Flavour Averaging Group (HFAG) [25] uses

$$CP_{\mathrm{HFAG}}|D^0\rangle=-|\bar{D}^0\rangle, \qquad (2.21)$$

which is the convention usually adopted for charm analyses. In the context of extracting γ from $B\to DK$ decays, it is usual practice to follow the "ADS" convention [15],

$$CP_{\mathrm{ADS}}|D^0\rangle=+|\bar{D}^0\rangle. \qquad (2.22)$$

The choice of convention affects several relevant parameters, which needs to be taken into account when providing charm input to the measurement of γ. The choice of convention decides how the mass eigenstates $|D_1\rangle$ and $|D_2\rangle$ defined in Eq. (2.1) relate to the *CP* even and odd eigenstates, $|D_+\rangle$ and $|D_-\rangle$. In the HFAG convention $|D_1\rangle\approx|D_-\rangle$ and $|D_2\rangle\approx|D_+\rangle$ (these relations become exact in the absence of CPV). In the ADS convention it is the other way around. The mixing variables x and y are defined in terms of (approximate) *CP* eigenstates, $x=\frac{M_+-M_-}{\Gamma}$, $y=\frac{\Gamma_+-\Gamma_-}{\Gamma}$, where the subscripts $+$ and $-$ label the masses and widths of the predominantly *CP*-even and *CP*-odd mass eigenstates, respectively. The formalism detailed above, with the mixing parameters defined in Eq. (2.3), follows the HFAG convention. Changing this to the ADS convention implies a simultaneous change $x\to-x$ and $y\to-y$.

The choice of convention also affects the complex interference parameter $\mathcal{Z}_{\Omega}^f$. To ensure that the same physical *CP* even or *CP* odd state corresponds to the same wave function (up to a phase), the $|D^0\rangle$ and $|\bar{D}^0\rangle$ wave functions in the two conventions must be related by
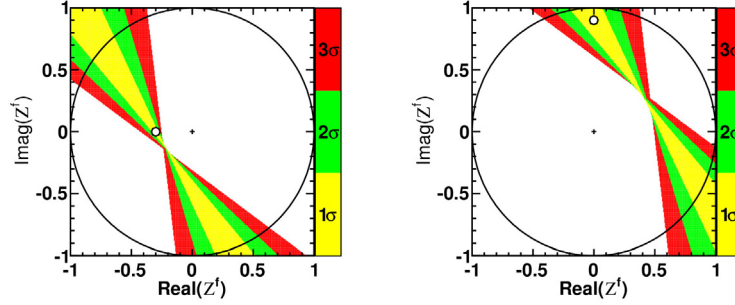
$$|D^0\rangle_{\mathrm{ADS}}=e^{i\xi}|D^0\rangle_{\mathrm{HFAG}},$$
$$|\bar{D}^0\rangle_{\mathrm{ADS}}=-e^{i\xi}|\bar{D}^0\rangle_{\mathrm{HFAG}}, \qquad (2.23)$$

where ξ is an arbitrary phase. As $\mathcal{Z}_{\Omega}^f\propto\int_{\Omega}\langle f_{\mathbf{p}}|\hat{H}|D^0\rangle\langle f_{\mathbf{p}}|\hat{H}|\bar{D}^0\rangle^*\frac{d\Phi}{d\mathbf{p}}\,d\mathbf{p}$, this implies

$$\mathcal{Z}_{\Omega\,\mathrm{ADS}}^f=-\mathcal{Z}_{\Omega\,\mathrm{HFAG}}^f, \qquad (2.24)$$

which is equivalent to

$$R_{D\,\mathrm{ADS}}^f=R_{D\,\mathrm{HFAG}}^f, \qquad c_i^{\mathrm{ADS}}=-c_i^{\mathrm{HFAG}},$$
$$\delta_{D\,\mathrm{ADS}}^f=\delta_{D\,\mathrm{HFAG}}^f+\pi, \qquad s_i^{\mathrm{ADS}}=-s_i^{\mathrm{HFAG}}. \qquad (2.25)$$

Fig. 1. Constraints on $\mathcal{Z}^f$ for $\mathcal{Z}^f = -0.3$ (left) and $\mathcal{Z}^f = 0.9i$ (right), taking into account current uncertainties on the mixing parameters x, y [30], but ignoring, in this illustration, other measurement uncertainties. The white filled circle in each plot indicates the central value of $\mathcal{Z}^f$ used.

3. Constraining the coherence factor and strong phase difference with D mixing

3.1. Overview

The dependence of Eqs. (2.11)–(2.14) on $\mathcal{Z}_\Omega^f$ has usually been taken to imply that external input on $\mathcal{Z}_\Omega^f$ is required to extract charm mixing parameters from multibody D decays [26–28]. Instead, we intend to use existing measurements of charm mixing parameters [19–25] as input, to constrain $\mathcal{Z}_\Omega^f$ from charm mixing in multibody decays [26]. This in turn provides important input to the amplitude model-unbiased measurement of γ [1–5,8]. So far, this type of input has only been accessible at the charm threshold [2–6].

In Eq. (2.19), the term linear in t (the "interference term") is sensitive to $y\,Re(\mathcal{Z}_\Omega^f) + x\,Im(\mathcal{Z}_\Omega^f)$, while in Eq. (2.20) it is sensitive to $y\,Re(\mathcal{Z}_\Omega^f) - x\,Im(\mathcal{Z}_\Omega^f)$, so both $Re\,\mathcal{Z}_\Omega^f$ and $Im\,\mathcal{Z}_\Omega^f$ can be extracted. However, previous studies [26] indicate that datasets much larger than those currently available are required to provide useful constraints on $\mathcal{Z}_{\Omega_i}^f$ (or c_i and s_i) from mixing using self-conjugate decays such as $D \to K_S\pi^+\pi^-$ and $D \to K_S K^+K^-$.

We will demonstrate here that significant improvements on $\mathcal{Z}^f$ can be achieved with existing data for the case where $D^0(t) \to f$ is a "wrong-sign" (WS) decay. This is a decay where $\mathcal{A}$ is a doubly Cabibbo-suppressed (DCS) amplitude, such as $D^0 \to K^+\pi^-\pi^+\pi^-$, or $D^0 \to K^+\pi^-\pi^0$. $\bar{D}^0(t) \to f$ is the corresponding "right-sign" (RS) decay, where $\mathcal{B}$ is Cabibbo-favoured (CF). In this case $\mathcal{A} \ll \mathcal{B}$. As a result, for typical decay times t, the interference term in the WS rate (Eq. (2.19)) is of a similar order of magnitude as the leading term, $\mathcal{A}^2$, providing enhanced sensitivity to $y\,Re(\mathcal{Z}_\Omega^f) + x\,Im(\mathcal{Z}_\Omega^f)$. On the other hand, for the RS rate (Eq. (2.20)), the constant term, $\mathcal{B}^2$, completely dominates the decay rate and there is effectively no sensitivity to $y\,Re(\mathcal{Z}_\Omega^f) - x\,Im(\mathcal{Z}_\Omega^f)$. In practice we will use the RS rate to normalise the WS rate, as this cancels many experimental uncertainties.

3.2. $\mathcal{Z}_\Omega^f$ from the mixing-induced interference of DCS and CF amplitudes

In this scenario it is useful to define the ratio of the DCS amplitude ($\mathcal{A}^{DCS}$) to the CF amplitude ($\mathcal{B}^{CF}$):

$$r_{Df} \equiv \frac{\mathcal{A}^{DCS}}{\mathcal{B}^{CF}}. \tag{3.1}$$

Neglecting terms of order 4 or higher in the small quantities x, y and r_{Df} results in the following expression for the ratio of WS to RS decays as a function of the D decay time t:

$$r_\Omega(t) = r_{Df}^2 + r_{Df}\big(y\,Re\,\mathcal{Z}_\Omega^f + x\,Im\,\mathcal{Z}_\Omega^f\big)\Gamma t + \frac{x^2 + y^2}{4}(\Gamma t)^2. \tag{3.2}$$

An analysis of the time-dependent decay rate ratio will, through the linear term of Eq. (3.2), provide a measurement of

$$b \equiv \big(y\,Re\,\mathcal{Z}_\Omega^f + x\,Im\,\mathcal{Z}_\Omega^f\big). \tag{3.3}$$

The factor r_{Df}, which also features in the linear term, can be obtained in the same analysis from the 0th order term of Eq. (3.2), and Γ has been measured very precisely [30]. Taking the D mixing parameters x and y as input, we can translate a measurement of b into constraints in the $Re\,\mathcal{Z}_\Omega^f - Im\,\mathcal{Z}_\Omega^f$ plane. A given value of b corresponds to a line of slope y/x in the $Re\,\mathcal{Z}_\Omega^f - Im\,\mathcal{Z}_\Omega^f$ plane defined by:

$$Im\,\mathcal{Z}_\Omega^f = -\frac{y}{x}\,Re\,\mathcal{Z}_\Omega^f + \frac{b}{x}. \tag{3.4}$$
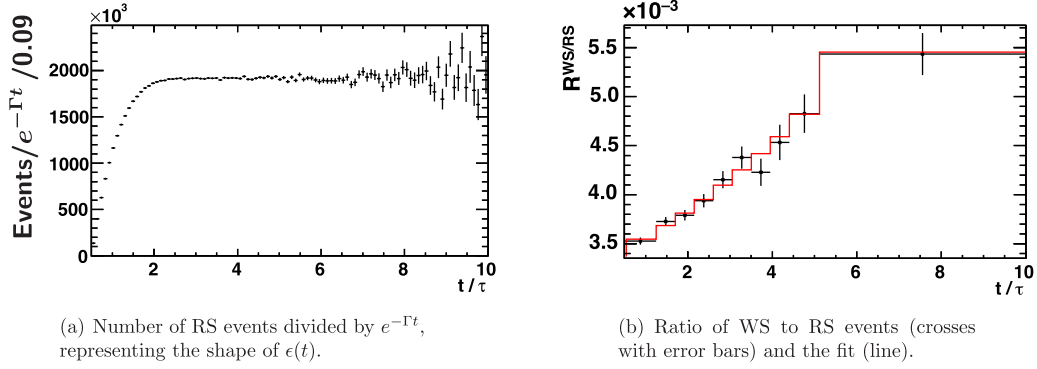
To show the effect of the current uncertainties in x and y on the measurement of $\mathcal{Z}^f$ from D mixing, we consider first the limiting case of negligible uncertainties on any other parameter, in particular on b defined in Eq. (3.3). We use the following values and uncertainties for x, y, and their correlation coefficient $\rho_{x,y}$ [25]:

$$x = (0.63 \pm 0.19)\%, \qquad y = (0.75 \pm 0.12)\%, \qquad \rho_{x,y} = 0.043. \tag{3.5}$$

Fig. 1 shows 1, 2 and 3σ confidence limits in the $Re\,\mathcal{Z}^f - Im\,\mathcal{Z}^f$ plane using these inputs for two illustrative example values for the complex interference parameter, $\mathcal{Z}^f = -0.3$ and $\mathcal{Z}^f = 0.9i$. The 1, 2 and 3σ regions are calculated using standard techniques based on χ^2 differences.

3.3. Sensitivity with existing LHCb datasets

To estimate the precision on $\mathcal{Z}^{K3\pi}$ achievable with current data, we perform a simulation study based on plausible $D \to K^+\pi^-\pi^+\pi^-$ event yields in LHCb's 3 fb^{-1} data sample taken in 2011 and 2012. We use the values for the mixing parameters given in Eq. (3.5), and $r_D = 0.058$ based on the WS to RS branching ratio reported in [30]. We generate simulated events according to the full expressions for the decay rates given in Eqs. (2.11)–(2.14). To take into account the effect of LHCb's trigger and event selection process, which preferentially selects decays with long D decay times, we apply a decay-time dependent efficiency function $\epsilon(t)$ based on that seen in [31]. For this feasibility study, we ignore other detector effects and background contamination. LHCb results for $D \to K^-\pi^+$ indicate that backgrounds can be controlled sufficiently well even for WS decays [24]. Based on the RS yields reported in [32], and taking into account that for the WS mode tighter selection criteria might be necessary to control backgrounds, we estimate about 8 million RS + WS events in LHCb's 2011–2012 dataset. The exact fraction of WS events depends on

(a) Number of RS events divided by $e^{-\Gamma t}$, representing the shape of $\epsilon(t)$.

(b) Ratio of WS to RS events (crosses with error bars) and the fit (line).

Fig. 2. Simulated data and fit in bins of proper decay time, expressed in units of $\tau = 1/\Gamma$. The discontinuous shape of the line representing the fit in (b) reflects the way the expected WS/RS ratio is calculated for each bin, described in the text.
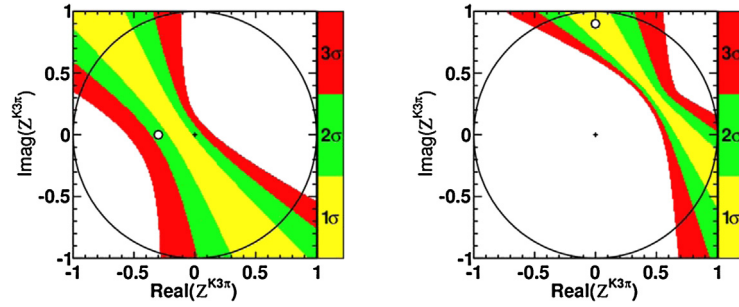
Fig. 3. Examples for constraints on $\mathcal{Z}^{K3\pi}$ obtained from 8 million simulated events, generated with $\mathcal{Z}^{K3\pi} = -0.3$ (left) and $\mathcal{Z}^{K3\pi} = 0.9i$ (right), with current uncertainties on x, y. The white filled circle indicates the value of $\mathcal{Z}^{K3\pi}$ used to generate the events.
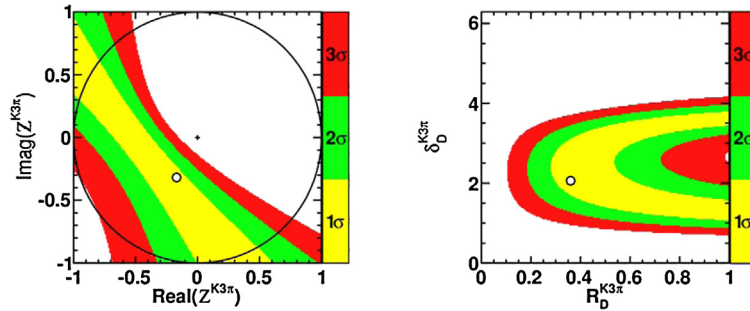
Fig. 4. Constraints on $\mathcal{Z}^{K3\pi}$ for $8M$ RS and $30k$ WS simulated events generated with CLEO-c's central value for the complex interference parameter, $\mathcal{Z}^{K3\pi} = -0.133 - 0.301 = 0.33e^{-1.99i}$ [5]. The constraints are shown both in Cartesian (left) and polar coordinates (right). The white filled circle indicates the values used to generate the events.

the input parameters, in particular on $R_D^{K3\pi}$; typically, 8 million RS + WS events correspond to about 30,000 WS events.

To constrain $\mathcal{Z}^{K3\pi}$ we perform a χ^2 fit to the WS/RS ratio in 10 bins of proper decay time. The bins have variable widths, chosen such that each bin contains a sufficient number of events. Using the same approximations that led to Eq. (3.2), we obtain for the expected WS to RS ratio $R_i^{WS/RS}$ in bin i that covers the proper decay time interval $[t_i^{min}, t_i^{max}]$:

$$R_i^{WS/RS}$$

$$= \frac{\int_{t_i^{min}}^{t_i^{max}} \epsilon(t) e^{-\Gamma t} \left(r_{Df}^2 + r_{Df} (y \operatorname{Re} \mathcal{Z}_\Omega^f + x \operatorname{Im} \mathcal{Z}_\Omega^f) \Gamma t + \frac{x^2 + y^2}{4} (\Gamma t)^2 \right) dt}{\int_{t_i^{min}}^{t_i^{max}} \epsilon(t) e^{-\Gamma t} \, dt}.$$

(3.6)

The fit parameters are r_{Df}, $b = y \operatorname{Re}(\mathcal{Z}_\Omega^f) + x \operatorname{Im}(\mathcal{Z}_\Omega^f)$, x, and y, where x and y are constrained according to Eq. (3.5).

In a real experiment, the time-dependent efficiency $\epsilon(t)$ would not necessarily be known a priory, but it is reasonable to assume that $\epsilon(t)$ would be the same for WS and RS decays. We therefore extract its shape from the (simulated) data by dividing the RS decay time distribution (histogrammed in 100 bins) by $e^{-\Gamma t}$, as shown in Fig. 2(a); the overall normalisation cancels when using $\epsilon(t)$ in Eq. (3.6).

A pull study based on generating and fitting 200 simulated data samples, each containing 8 million RS + WS events, shows no evidence of fit biases, and confirms the correct coverage of the confidence intervals obtained from the fit χ^2.

An example of such a fit is shown in Fig. 2(b). The $8M$ events have been generated using CLEO-c's central value $\mathcal{Z}^{K3\pi} = -0.133 - 0.301i$ [5] and include $30.5k$ WS events. Fig. 3 shows 1, 2 and 3σ confidence regions based on 8 million simulated events that have been generated with the illustrative values $\mathcal{Z}^{K3\pi} = -0.3$ and $\mathcal{Z}^{K3\pi} = 0.9i$ used also to obtain Fig. 1. Fig. 4 shows the constraints for events generated using the CLEO-c central value for $\mathcal{Z}^{K3\pi}$, in both polar coordinates (i.e. the coherence factor
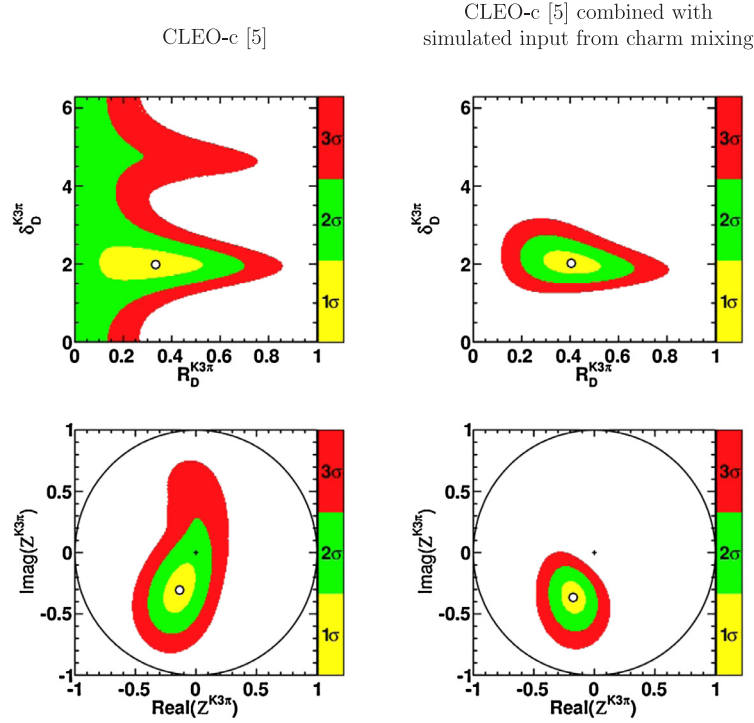
Fig. 5. Constraints on $\mathcal{Z}^{K3\pi}$ obtained by CLEO-c [5] are shown on the left. Constraints obtained by combining the CLEO-c results with the input from simulated $D \to K^+\pi^-\pi^+\pi^-$ charm mixing data are shown on the right. The simulated signal sample is similar in size to that expected from 3 fb^{-1} of data taken by LHCb in 2011 and 2012. The same results are shown in polar coordinates $R_D^{K3\pi}$, $\delta_D^{K3\pi}$ (top row) and in Cartesian coordinates $Re\,\mathcal{Z}^{K3\pi}$, $Im\,\mathcal{Z}^{K3\pi}$ (bottom row). The white filled circle indicates the location with the smallest χ^2.

Table 1
Constraints on $R_D^{K3\pi}$ and $\delta_D^{K3\pi}$ as well as $Re\,\mathcal{Z}^{K3\pi}$ and $Im\,\mathcal{Z}^{K3\pi}$ from simulation, CLEO-c [5], and their combination, at 68% and 95% CL, obtained with two different techniques following [5], as described in the text. The $\Delta\chi^2$ method is not suitable for obtaining separate constraints on $Re\,\mathcal{Z}^{K3\pi}$ and $Im\,\mathcal{Z}^{K3\pi}$ from the simulated mixing data alone.

	Simulation 8M evts	CLEO-c [5]	Combination
Fit result (where available) with 68% confidence intervals ($\Delta\chi^2$)			
$R_D^{K3\pi}$	[0.28, 1.00]	$0.33^{+0.20}_{-0.23}$	$0.40^{+0.13}_{-0.11}$
$\delta_D^{K3\pi}$	[1.07, 3.77]	$1.99^{+0.46}_{-0.42}$	$2.03^{+0.33}_{-0.27}$
$Re\,\mathcal{Z}^{K3\pi}$	–	$-0.14^{+0.14}_{-0.14}$	$-0.18^{+0.11}_{-0.10}$
$Im\,\mathcal{Z}^{K3\pi}$	–	$-0.31^{+0.23}_{-0.19}$	$-0.37^{+0.14}_{-0.14}$
Bayesian 95% confidence intervals			
$R_D^{K3\pi}$	[0.27, 1.00]	[0.00, 0.63]	[0.20, 0.66]
$\delta_D^{K3\pi}$	[1.07, 3.83]	–	[1.51, 2.77]
$Re\,\mathcal{Z}^{K3\pi}$	[−0.96, 0.50]	[−0.41, 0.13]	[−0.39, 0.03]
$Im\,\mathcal{Z}^{K3\pi}$	[−0.58, 1.00]	[−0.69, 0.41]	[−0.65, −0.11]

$R_D^{K3\pi} = |\mathcal{Z}^{K3\pi}|$ and strong phase difference $\delta_D^{K3\pi} = -\arg(\mathcal{Z}^{K3\pi})$) and Cartesian coordinates ($Re\,\mathcal{Z}^{K3\pi}$ and $Im\,\mathcal{Z}^{K3\pi}$).

To evaluate the potential impact of input from charm mixing on the precision of $\mathcal{Z}^{K3\pi}$, we combine the χ^2 function used to obtain Fig. 4 with CLEO-c's measurement of $\mathcal{Z}^{K3\pi}$ [5]. The CLEO-c results, and the combination with our simulated data, are shown in Fig. 5. The input from charm mixing improves the constraints considerably. The effect is particularly striking at the $\geqslant 2\sigma$ level where there were previously no constraints on δ_D^f. To quantify these improvements, one-dimensional 68% and 95% confidence intervals for $R_D^{K3\pi}$ and $\delta_D^{K3\pi}$ are calculated, following the same procedures as used by CLEO-c [5] to ensure comparable results. The 68% confidence limits are based on a standard χ^2 difference calculation. The same process would lead to 95% confidence limits

reaching the edge of the R_D^f–δ_D^f parameter space in the CLEO-c measurement. These are therefore obtained using a Bayesian approach with a uniform prior in the physically allowed region of the parameter of interest. The results are summarised in Table 1. The constraints from our 8M simulated charm events (with 30k WS events) shrink the existing uncertainties on $Re\,\mathcal{Z}^{K3\pi}$ and $Im\,\mathcal{Z}^{K3\pi}$ by a factor of ~ 1.5, and the 95% CL on $Im\,\mathcal{Z}^{K3\pi}$ by a factor of two. In terms of polar coordinates, the simulated input approximately halves the uncertainty in $R_D^{K3\pi}$, and significantly reduces the uncertainty on $\delta_D^{K3\pi}$. There is currently no constraint on $\delta_D^{K3\pi}$ at the 2σ level, and only a one-sided upper limit for $R_D^{K3\pi}$. From the combination of our simulated data with the CLEO-c result, we obtain $\delta_D^{K3\pi} \in [1.51, 2.77]$, and $R_D^{K3\pi} \in [0.20, 0.66]$ at 95% confidence.

4. Conclusion

Charm mixing is sensitive to the same charm interference parameters that are relevant to the measurement of γ in $B^\pm \to DK^\pm$ and related decay modes [1,7–9,26–28]. So far, these have only been accessible at the charm threshold [2–6]. The increased precision with which the charm mixing parameters x and y have been measured [6,19–25] opens up the possibility of constraining charm interference parameters using charm mixing. However, previous studies indicate that for decays to self-conjugate final states, such as $D \to K_S \pi^+\pi^-$ and $D \to K_S K^+ K^-$, datasets much larger than those currently available are required to significantly improve constraints on the binned complex interference parameters $\mathcal{Z}^f_{\Omega_i} = c_i + is_i$ from charm mixing [26]. On the other hand, in wrong-sign decay modes such as $D^0 \to K^+\pi^-\pi^+\pi^-$ and $D^0 \to K^+\pi^-\pi^0$, the mixing-induced interference effects are significantly enhanced compared to self-conjugate decays. This provides greater sensitivity to the complex interference parameter $\mathcal{Z}^f$, or, equivalently, the

coherence factor $R_D^f = |\mathcal{Z}^f|$ and average strong phase difference $\delta_D^f = -\arg(\mathcal{Z}^f)$ introduced in [1]. While it is interesting to note that useful information can be obtained in this way without additional input, the true power of the method lies in the combination with threshold data. We evaluate the potential of this approach with a simulation study based on estimated $D \to K^+\pi^-\pi^+\pi^-$ signal yields expected in LHCb's 2011 and 2012 dataset. We do not assume any improvements on external inputs. Our results indicate that charm mixing input from existing LHCb data, when combined with CLEO-c's measurement [5], could substantially reduce the current uncertainty on the coherence factor and average strong phase difference in $D \to K^+\pi^-\pi^+\pi^-$. Such a measurement can be expected to have a significant impact on the precision with which the CKM parameter γ can be measured at LHCb, BELLE II, and the LHCb upgrade.

Acknowledgements

References

[1] D. Atwood, A. Soni, Role of charm factory in extracting CKM phase information via $B \to DK$, Phys. Rev. D 68 (2003) 033003, http://dx.doi.org/10.1103/PhysRevD.68.033003, arXiv:hep-ph/0304085.

[2] J. Libby, et al., Model-independent determination of the strong-phase difference between D^0 and $\bar{D}^0 \to K^0_{S,L}h^+h^-$ ($h = \pi, K$) and its impact on the measurement of the CKM angle γ/ϕ_3, Phys. Rev. D 82 (2010) 112006, http://dx.doi.org/10.1103/PhysRevD.82.112006, arXiv:1010.2817.

[3] R.A. Briere, et al., First model-independent determination of the relative strong phase between D^0 and $\bar{D}^0 \to K^0_S\pi^+\pi^-$ and its impact on the CKM Angle γ/ϕ_3 measurement, Phys. Rev. D 80 (2009) 032002, http://dx.doi.org/10.1103/PhysRevD.80.032002, arXiv:0903.1681.

[4] J. Insler, et al., Studies of the decays $D^0 \to K^0_S K^-\pi^+$ and $D^0 \to K^0_S K^+\pi^-$, Phys. Rev. D 85 (2012) 092016, http://dx.doi.org/10.1103/PhysRevD.85.092016, arXiv:1203.3804.

[5] N. Lowrey, et al., Determination of the $D^0 \to K^-\pi^+\pi^0$ and $D^0 \to K^-\pi^+\pi^+\pi^-$ coherence factors and average strong-phase differences using quantum-correlated measurements, Phys. Rev. D 80 (2009) 031105, http://dx.doi.org/10.1103/PhysRevD.80.031105, arXiv:0903.4853.

[6] D.M. Asner, et al., Determination of the $D^0 \to K^+\pi^-$ relative strong phase using quantum-correlated measurements in $e^+e^- \to D^0\bar{D}^0$ at CLEO, Phys. Rev. D 78 (2008) 012001, http://dx.doi.org/10.1103/PhysRevD.78.012001, arXiv:0802.2268.

[7] J. Lees, et al., Search for $b \to u$ transitions in $B^\pm \to [K^\mp\pi^\pm\pi^0]_D K^\pm$ decays, Phys. Rev. D 84 (2011) 012002, http://dx.doi.org/10.1103/PhysRevD.84.012002, arXiv:1104.4472.

[8] A. Giri, Y. Grossman, A. Soffer, J. Zupan, Determining γ using $B^\pm \to DK^\pm$ with multibody D decays, Phys. Rev. D 68 (2003) 054018, http://dx.doi.org/10.1103/PhysRevD.68.054018, arXiv:hep-ph/0303187.

[9] R. Aaij, et al., A model-independent Dalitz plot analysis of $B^\pm \to DK^\pm$ with $D \to K^0_S h^+h^-$ ($h = \pi, K$) decays and constraints on the CKM angle γ, Phys. Lett. B 718 (2012) 43–55, http://dx.doi.org/10.1016/j.physletb.2012.10.020, arXiv:1209.5869.

[10] A measurement of γ from a combination of $B^\pm \to DK^\pm$ analyses including first results using $2fb^{-1}$ of 2012 data (LHCb-CONF-2013-006).

[11] R. Aaij, et al., A measurement of γ from a combination of $B^\pm \to Dh^\pm$ analyses, Phys. Lett. B (2013), submitted for publication, arXiv:1305.2050.

[12] R. Aaij, et al., Observation of the suppressed ADS modes $B^\pm \to [\pi^\pm K^\mp\pi^+\pi^-]_D K^\pm$ and $B^\pm \to [\pi^\pm K^\mp\pi^+\pi^-]_D\pi^\pm$, Phys. Lett. B 723 (2013) 44, http://dx.doi.org/10.1016/j.physletb.2013.05.009, arXiv:1303.4646.

[13] M. Gronau, D. Wyler, On determining a weak phase from CP asymmetries in charged B decays, Phys. Lett. B 265 (1991) 172–176, http://dx.doi.org/10.1016/0370-2693(91)90034-N.

[14] M. Gronau, D. London, How to determine all the angles of the unitarity triangle from $B_d \to DK_S$ and $B_s^0 \to D\phi$, Phys. Lett. B 253 (1991) 483–488, http://dx.doi.org/10.1016/0370-2693(91)91756-L.

[15] D. Atwood, I. Dunietz, A. Soni, Enhanced CP violation with $B \to KD^0(\bar{D}^0)$ modes and extraction of the Cabibbo–Kobayashi–Maskawa angle γ, Phys. Rev. Lett. 78 (1997) 3257–3260, http://dx.doi.org/10.1103/PhysRevLett.78.3257.

[16] A. Giri, Y. Grossman, A. Soffer, J. Zupan, Determining γ using $B^\pm \to DK^\pm$ with multibody D decays, Phys. Rev. D 68 (2003) 054018, http://dx.doi.org/10.1103/PhysRevD.68.054018.

[17] A. Poluektov, et al., Measurement of ϕ_3 with Dalitz plot analysis of $B^\pm \to D^{(*)}K^\pm$ decays, Phys. Rev. D 70 (2004) 072003, http://dx.doi.org/10.1103/PhysRevD.70.072003.

[18] J. Rademacker, G. Wilkinson, Determining the unitarity triangle γ with a four-body amplitude analysis of $B^+ \to (K^+K^-\pi^+\pi^-)_D K^\pm$ decays, Phys. Lett. B 647 (2007) 400–404, http://dx.doi.org/10.1016/j.physletb.2007.01.071, arXiv:hep-ph/0611272.

[19] T. Aaltonen, et al., Evidence for D^0–$\bar{D}^0$ mixing using the CDF II detector, Phys. Rev. Lett. 100 (2008) 121802, http://dx.doi.org/10.1103/PhysRevLett.100.121802, arXiv:0712.1567.

[20] M. Staric, et al., Evidence for D^0–$\bar{D}^0$ mixing, Phys. Rev. Lett. 98 (2007) 211803, http://dx.doi.org/10.1103/PhysRevLett.98.211803, arXiv:hep-ex/0703036.

[21] B. Aubert, et al., Evidence for D^0–$\bar{D}^0$ mixing, Phys. Rev. Lett. 98 (2007) 211802, http://dx.doi.org/10.1103/PhysRevLett.98.211802, arXiv:hep-ex/0703020.

[22] B. Aubert, et al., Measurement of D^0–$\bar{D}^0$ mixing from a time-dependent amplitude analysis of $D^0 \to K^+\pi^-\pi^0$ decays, Phys. Rev. D 103 (2009) 211801, http://dx.doi.org/10.1103/PhysRevD.103.211801, arXiv:0807.4544.

[23] B. Aubert, et al., Measurement of D^0–$\bar{D}^0$ mixing using the ratio of lifetimes for the decays $D^0 \to K^-\pi^+$ and K^+K^-, Phys. Rev. D 80 (2009) 071103, http://dx.doi.org/10.1103/PhysRevD.80.071103, arXiv:0908.0761.

[24] R. Aaij, et al., Observation of D^0–$\bar{D}^0$ oscillations, Phys. Rev. Lett. 110 (2013) 101802, http://dx.doi.org/10.1103/PhysRevLett.110.101802, arXiv:1211.1230.

[25] Y. Amhis, et al., Averages of B-Hadron, C-Hadron, and tau-lepton properties as of early 2012, arXiv:1207.1158.

[26] C. Thomas, G. Wilkinson, Model-independent D^0–$\bar{D}^0$ mixing and CP violation studies with $D^0 \to K^0_S\pi^+\pi^-$ and $D^0 \to K^0_S K^+K^-$, J. High Energy Phys. 1210 (2012) 185, http://dx.doi.org/10.1007/JHEP10(2012)185, arXiv:1209.0172.

[27] S. Malde, G. Wilkinson, D^0–$\bar{D}^0$ mixing studies with the decays $D^0 \to K^0_S K^\mp\pi^\pm$, Phys. Lett. B 701 (2011) 353–356, http://dx.doi.org/10.1016/j.physletb.2011.05.072, arXiv:1104.2731.

[28] A. Bondar, A. Poluektov, V. Vorobiev, Charm mixing in the model-independent analysis of correlated $D^0 \bar{D}^0$ decays, Phys. Rev. D 82 (2010) 034033, http://dx.doi.org/10.1103/PhysRevD.82.034033, arXiv:1004.2350.

[29] I. Adachi, First measurement of ϕ_3 with a binned model-independent Dalitz plot analysis of $B^\pm \to DK^\pm$, $D \to K^0_S\pi^+\pi^-$ decay, arXiv:1106.4046.

[30] J. Beringer, et al., Review of particle physics, Phys. Rev. D 86 (2012) 010001, http://dx.doi.org/10.1103/PhysRevD.86.010001.

[31] R. Aaij, et al., Measurement of mixing and CP violation parameters in two-body charm decays, J. High Energy Phys. 4 (2012) 129, http://dx.doi.org/10.1007/JHEP04(2012)129, arXiv:1112.4698.

[32] R. Aaij, et al., Model-independent search for CP violation in $D^0 \to K^-K^+\pi^-\pi^+$ and $D^0 \to \pi^-\pi^+\pi^+\pi^-$ decays, Phys. Lett. B 726 (2013) 623–633, http://dx.doi.org/10.1016/j.physletb.2013.09.011, arXiv:1308.3189.